Journal of Stress Analysis
Vol. 9, No. 1, 2025, 37-49
Bu-Ali Sina University

ORIGINAL RESEARCH PAPER

Using the Hot-Spot Determination Concept to Predict Fatigue Failure of Notched Components in the Presence of Residual Stress Fields

Rahman Seifi*, Mohammad Reza Mohammadi
Department of Mechanical Engineering, Faculty of Engineering, Bu-Ali Sina University, Hamedan, Iran.

Article info

Article history:
Received 11 March 2025
Received in revised form
19 May 2025
Accepted 26 June 2025

Keywords:
Fatigue life
Notched components
Hot-spot determination
Residual stress

Abstract

The aim of this study is to introduce a new method for predicting fatigue failure in notched specimens under residual stress fields. The proposed model is based on a hot-spot determination and the local stress ratio around the notch root to estimate fatigue life. This concept aims to assess the influence of the plastic zone on the fatigue process within a limited volume near the notch root, which governs fatigue failure. To verify the accuracy and validity of the method, experiments were conducted on various notched specimens. Both U- and V- notched specimens with a wide range of elastic stress concentration factors were systematically investigated. A finite element model with a refined mesh around the notch root was employed to determine the stress distribution. The results showed acceptable agreement between the predictions and experimental data, confirming the model's effectiveness. Additionally, the model demonstrated suitable stability in predicting the fatigue lives for notches with high stress concentrations. This approach significantly simplifies and improves the accuracy of fatigue predictions for notched components, particularly when residual stress fields are considered. Another key advantage of the proposed model is its ability to correlate fatigue predictions with experimental results from simple specimens, data for which are typically readily available in engineering databases.

Nomenclature

a_v	Hot spot distance from notch root	K_G	Notch geometry factor
R	Stress ratio	R_{local}	Local stress ratio
R_{nom}	Nominal (applied stress ratio)	SCF	Stress concentration factor
σ_a	Stress amplitude	σ_m	Mean stress
$\sigma_{m,app}$	Applied mean stress	$\sigma_{r,yy}$	Residual stress in hot spot location

1. Introduction

Fatigue has been one of the most significant causes of structural failures over the past century. Extensive research has been conducted to investigate the factors influencing fatigue failure and to ensure safe structural designs. Due to the complexity of fatigue mechanisms, studies have been divided into numerous specialized fields, often making it difficult to establish

*Corresponding author: R. Seifi (Professor)
E-mail address: rahmanseifi@yahoo.com
10.22084/jrstan.2025.30956.1267
ISSN: 2588-2597

connections between them. Some of these studies, particularly those focused on fatigue life prediction, have been reviewed in some state-of-the-art publications [1, 2]. A survey of existing research suggests that developing a unifying theory capable of predicting fatigue under diverse conditions remains highly challenging. One of the most debated topics in fatigue failure is the effect of stress raisers, commonly referred to as notches. Notches significantly reduce the fatigue life of a component compared to smooth specimens. Traditional methods for predicting fatigue failure in notched components rely on notch sensitivity and correction factors. However, since this approach depends on numerous parameters typically determined through experimentation, it remains largely empirical. Widely used in mechanical design, this method is described in detail in machine design texts[3]. Numerous analytical methods have also been developed to predict fatigue failure in notched components. Some of these theories have been classified and discussed recently in a book [4]. Over the past two decades, particular attention has been paid to theories based on length parameters. The pioneering work in this field is often attributed to Neuber [5] and Peterson [6]. Neuber's method calculates the average elastic stress over a characteristic distance from the notch root, whereas Peterson's approach focuses on stresses at a specific distance. These distances were defined based on material properties and determined experimentally. Both methods have been systematically evaluated and compared in two recent references [4, 7] to assess their accuracy and applicability under different conditions. The findings suggest that both methods exhibit similar levels of accuracy and conservatism, though their performance may vary depending on the specific scenario. In recent years, a new theory has been proposed and developed, utilizing stress analysis to determine the length parameter [8-10]. Other theories incorporate improved length parameters, such as those based on surface or volume effects. Thanks to significant advancements in computational technology and numerical methods, these approaches have become more practical today than they were three decades ago. Some of these methods have been introduced and compared with Neuber's and Peterson's theories [4].

Fatigue life evaluation of notched components is a critical aspect of ensuring structural integrity, especially under the influence of residual stresses. Various methods have been developed and applied to improve fatigue life prediction accuracy under different loading and environmental conditions. A prominent approach used in several studies is the theory of critical distance (TCD). The elastoplastic form of TCD, particularly the point method (PM), was shown to be effective in predicting fatigue life under variable amplitude (VA) loading conditions in notched components, offering a material-based critical length that remains constant regardless of the notch severity or load profile variations [11]. Similarly, the equivalent virtual stress (EVS) method combined with TCD's PM and line method (LM) was applied to account for overload-induced residual stresses. This combination showed reliable predictions for both U- and V-notched specimens, with LM yielding more accurate results when the critical distance is farther from the notch root [12]. Furthermore, TCD was extended to impact fatigue scenarios by incorporating mean strain modification, proving successful in predicting the fatigue life under low-velocity repeated impacts [13].

Several methods focused explicitly on the residual stress effects. One study developed a fatigue life estimation method based on the mean stress distribution and local stress ratio around the notch, accounting for plastic strains due to overload, and found strong agreement with experimental results for notches of varying severity [14]. Another work introduced a compliance-based correction method for fatigue crack growth data, effectively compensating for variability in the residual stress fields in additively manufactured specimens [15]. Additionally, the influence of the residual stress on V-notched components was reviewed, highlighting the role of the notch stress intensity factor and its evolution during the fatigue loading [16].

Finite element analysis has also been leveraged to assess the influence of the residual stresses. One study combined standard S–N curve data, fracture mechanics, and the ANSYS SMART crack growth model to assess components with induced compressive residual stress. The method effectively distinguished between crack initiation and propagation phases, improving fatigue life estimation accuracy [17]. Similarly, the residual stress induced by the welding process was incorporated into the fatigue crack propagation models using superposition of stress intensity factors, accurately reflecting the crack growth behavior in stiffened panels [18].

Advanced modeling techniques have also emerged. A non-local, strain-based finite fracture mechanics approach was proposed for additively manufactured notched samples, considering both strain requirements and energy balance. This method outperformed both classical TCD and finite fracture mechanics in prediction accuracy [19]. Another study proposed a non-local model incorporating stress/strain gradients and elastic-plastic damage using critical plane and triaxiality methods, successfully predicting the fatigue damage evolution [20].

Multiaxial loading scenarios have received attention through methods like the energy-based critical plane method, where factors such as non-proportional hardening and stress gradients were integrated into a modified Manson–Coffin-based life prediction model [21]. Similarly, a two-point method combining TCD and stress–distance normalization was applied for fatigue prediction under multiaxial cyclic loads, showing

higher accuracy than traditional local approaches [22].

Machine learning techniques have also been employed. A hybrid model combining long short-term memory (LSTM) and feedforward neural networks was proposed to simulate multiaxial fatigue in automotive components under non-stationary loads, enabling faster predictions with minimal loss of accuracy compared to finite element results [23].

In terms of service-specific studies, fatigue life under hydrogen environments has been explored extensively. Full-scale fatigue testing of pipelines exposed to hydrogen highlighted the significance of crack initiation in total life and developed S–N curve families for practical integrity assessments [24]. Another study applied lifecycle fatigue analysis to hydrogen pipelines, incorporating stress conditions and using both conventional S–N and linear elastic fracture mechanics methods [25]. These insights are critical for emerging energy storage infrastructures, such as hydrogen pipelines [26].

Plasticity effects under complex loading, such as fretting fatigue, were also modeled using a combination of TCD for crack initiation and Kujawski's parameter for propagation, indicating the importance of elastoplastic assumptions for improved predictions [27].

Lastly, models with broad applicability were proposed, including a stress-based fatigue life prediction model suitable for all life stages and complex stress states. This model incorporates stress ratio and gradient corrections, showing superior performance over traditional strain-life models [28]. Residual life prediction integrated with surface remanufacturing techniques also provided a practical approach for automotive components, using X-ray diffraction and repair strategies tailored to local damage and stress distributions [29].

Despite considerable progress in length-parameter-based prediction methods, many approaches still face limitations, particularly when dealing with the residual stress fields near the notch root. At the same time, the influence of the residual stress cannot be overlooked, as it plays a crucial role in the fatigue failure. In this study, a new model based on a characteristic length is proposed to estimate the effect of the residual stress fields around the notch root on the fatigue failure. The material selected for investigation was AA 2024-T3, chosen for its high fatigue resistance and widespread use in aircraft fuselages and wings. The model's accuracy and validity were confirmed through experimental tests on various notch geometries with significantly different stress concentration factors (SCFs).

1.1. Hot-Spot Determination

The fatigue life of metallic materials is significantly influenced by the stress ratio (R). This parameter governs the mean stress level and has a profound effect on the initiation and propagation of fatigue cracks.

When the stress ratio is negative (R=-1), the loading is fully reversed, which tends to be more damaging due to the alternating tensile and compressive stresses. As the stress ratio increases, the mean stress also increases, particularly when the maximum stress is tensile. An increase in mean tensile stress generally reduces the fatigue life due to enhanced crack opening and propagation, while a compressive mean stress (e.g., compressive residual stress) can improve fatigue resistance by reducing the stress intensity factor range and retarding the crack growth.

The effect of the stress ratio is also material-dependent. For example, high-strength steels are more sensitive to mean stress variations than aluminum alloys. Additionally, surface treatments, residual stresses, and environmental factors can modify the way stress ratio influences fatigue behavior.

It has also been shown that negative mean stress has little to no effect on the fatigue endurance limit in ductile materials, while in brittle materials, it tends to increase the endurance limit [3]. Moreover, when a crack exists in a material and negative mean stress is applied, the duration for which the crack remains open during a loading cycle is reduced. As a result, crack growth slows down, thereby increasing the fatigue life. Based on this reasoning, it is plausible to identify a region within a component containing residual compressive stresses where the stress ratio reaches a minimum value. In this study, this concept is applied to a notched specimen in the region affected by residual stress induced by an overload. Since in notched components, the maximum stress (both applied and residual) is typically concentrated perpendicular to the notch axis and near its root, efforts have been made to determine the mean stress and stress amplitude at the point with the minimum stress ratio, based on the applied load and the residual stress distribution caused by the overload. The fatigue life is then evaluated accordingly. A schematic of the concept and variations of the stresses and stress ratios is shown in Fig. 1.

This assumption significantly simplifies the analysis of the fatigue mechanism around the notch root. Similar approaches have been adopted in previous studies [9, 30-32]. The introduction of a hot spot is an attempt to approximate the behavior of the limited volume of plastically deformed material near the notch root, circumventing the complexities associated with the actual material response.

This approach to fatigue failure prediction can be considered a method based on the length parameters. Regardless of the varying terminology used by other authors, fatigue prediction methods relying on length parameters will be collectively referred to as characteristic length methods in this study. This assertion aligns closely with the definition of length parameters employed by other researchers to estimate the fatigue failure in notched components [10, 30, 33, 34].

Over the past three decades, various characteristic length methods have been developed, enabling the use of both stress distribution fields and material properties to define the characteristic length. Since this study focuses on the residual stress field, the definition is based on the stress distribution around the notch root.

Stress magnitude and stress ratio are two critical parameters governing the fatigue mechanism in both notched and plain specimens. To the authors' knowledge, most prediction methods prioritize stress while simplifying the local stress ratio (R_{local}), often assuming it remains constant or equal to the nominal stress ratio (R_{nom}). However, in the presence of a residual stress field, R_{local} cannot be treated as constant, leading to challenges in accounting for its influence on the fatigue behavior. For this reason, the presented method places greater emphasis on R_{local}. It is hypothesized that the hot spot location corresponds to the location where R_{local} reaches its minimum value. Although this definition simplifies the problem's conditions, it will later be demonstrated to be surprisingly accurate and stable in predicting the fatigue life of the notched components under residual stresses.

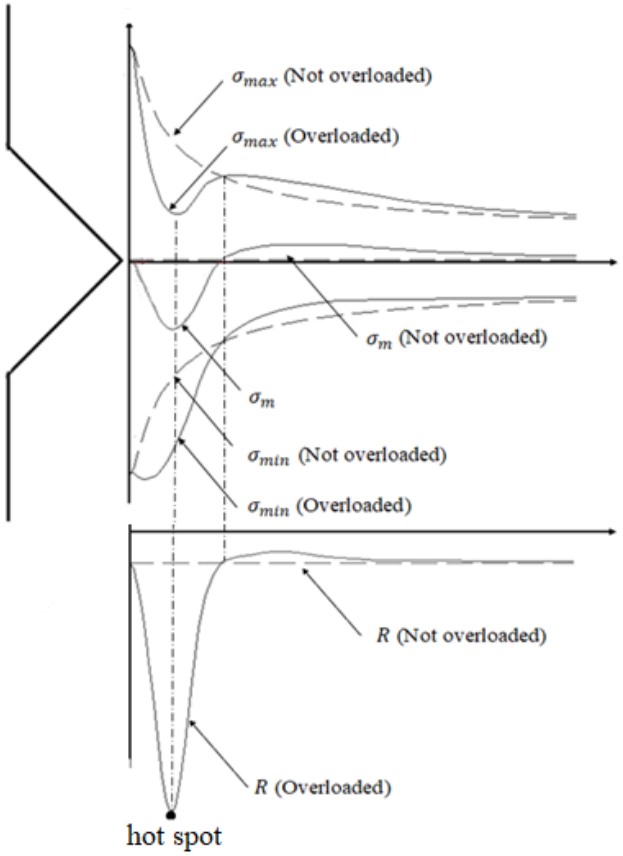

Fig. 1. A schematic of the hot spot concept and variations of the stresses and stress ratios.

Based on the above explanations, the hot-spot location can be mathematically defined by Equation 1 as follows:

$$a_v = a(R_{local,min}) \tag{1}$$

Where a_v is the distance of the location from the notch root and $a\,(R_{local})$ is the distribution on the local stress ratio versus distance from notch root.

1.2. Prediction Method

To apply the proposed method for fatigue prediction, the effective stress parameters must first be computed. The stress component σ_{yy} (acting along the loading direction and perpendicular to the notch axis) was selected as the effective stress parameter. In this scenario, σ_{yy} represents the maximum in-plane principal stress.

The mean stress (σ_m) can be determined using Eq. 2, incorporating the residual stress distribution (σ_r) around the notch root [35, 36]:

$$\sigma_m = \sigma_{r,yy} + \sigma_{m,app} \tag{2}$$

Where $\sigma_{m,app}$ is the induced mean stress at the hot spot due to the applied load. Meanwhile, the maximum stress (σ_{max}) is derived from the final stress value at the hot spot location when the external load reaches its peak value.

Direct application of Eq. 1 in its current form is challenging due to the limited published data on the fatigue failures at stress ratios smaller than -1. This scarcity of information at extremely low R-values likely stems from researchers' predominant focus on nominal stress ratios (R_{nom}).

Analysis of the S-N curve for AA 2024-T3 [37] and results reported in other studies[38, 39] reveals that the influence of R_{nom} on the fatigue mechanisms progressively diminishes as it decreases below zero. Consequently, stress ratios R<-1 exhibit relatively minor effects on the fatigue failure compared to higher R_{nom} values. Under overload conditions (as in the present study), significant compressive residual stresses develop near the notch root due to substantial plastic deformation in this region. This leads to two key observations: (i) The stress condition satisfies $(\sigma_{max} - \sigma_m) > (\sigma_m - \sigma_{min})$, and (ii) the local stress ratio at the notch root falls within $-1 < R_{local} < 0$.

As compressive residual stresses attenuate with increasing distance from the notch root, R_{local} decreases progressively. Thus, regions with $R_{local} > -1$ occur farther from the notch root than points where $R_{local} = -1$. This spatial variation suggests that the effect of $R_{local} > -1$ becomes even less pronounced than the values typically reported for plain specimens.

Given the limited data available for R<-1 and its expected minimal influence on the fatigue life of notched components in this study, the parameter a_v was estimated using the first minimum occurrence of

R_{local}. This approach offers some advantages: it enables the use of stress amplitude (σ_a) under fully reversed loading conditions, simplifying analysis; it facilitates computations by leveraging readily available reference charts from engineering handbooks and manuals; and it allows direct comparison of the loading condition effects on the effective stress parameters.

The stress amplitude at the hot spot, termed the effective stress amplitude ($\sigma_{a,eff}$), cannot be directly used for the fatigue failure estimation. This limitation arises because the small size of the hot spot makes it susceptible to influences from both notch geometry and alterations in stress flow. To account for these effects, the impact of the notch geometry on the fatigue behavior was incorporated directly into $\sigma_{a,eff}$. Based on experimental evaluation in this study, this influence was quantified via a notch geometry factor (K_G), applied multiplicatively to $\sigma_{a,eff}$ as follows:

$$s_a = K_G s_{a,eff} \tag{3}$$

Here, s_a represents the stress amplitude in a plain specimen exhibiting equivalent fatigue life.

This equation establishes a relationship between the stress parameter in a notched component (including residual stress effects) and the nominal stress in a simple specimen. While this approach provides a practical solution, future research should focus on developing analytical methods to determine effects of notch geometry on $\sigma_{a,eff}$ without relying on the experimental approximations. The methodology for deriving K_G will be comprehensively explained and discussed in the following sections.

2. Experimental procedure

To evaluate the accuracy and reliability of the proposed concept, experimental tests were conducted on specimens with various notch geometries under different loading conditions. Fig. 2 presents detailed illustrations of the investigated notch geometries, along with their corresponding elastic stress concentration factors (SCFs). These SCFs were determined using finite element (FE) analysis under tensile loading conditions.

The present study employed AA 2024-T3 aluminum alloy sheets with a thickness of 3mm, a material widely recognized for its excellent fatigue resistance properties. The chemical composition of the alloy is provided in Table 1.

Microstructural analysis revealed an average grain size of 28μm, determined in accordance with ASTM E112 [41]. The mechanical properties of the alloy, summarized in Table 2, were derived from stress-strain curves obtained through standard tensile testing performed on a SANTAM tensile testing machine, following ASTM E8 [42] specifications. The corresponding stress-strain curve and tensile test specimen geometry are illustrated in Fig. 3.

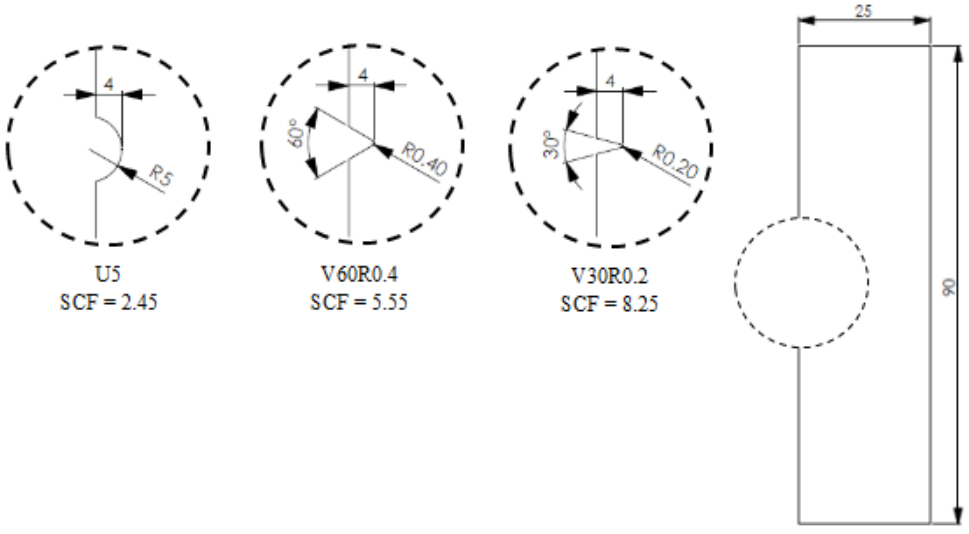

Fig. 2. Geometry of notched specimens.

Table 1
Chemical composition of AA 2024-T3.

Element	Al	Si	Fe	Cu	Mn	Mg
AA 2024 [40]	Base	0.07	0.12	4.44	0.51	1.52
Sample	Base	Max 0.5	Max 0.5	3.8-4.9	0.3-0.9	1.2-1.8
Element	Cr	Ni	Zn	Ti	Zr	
AA 2024 [40]	<0.01	0.01	0.03	0.04	<0.01	
Sample	Max 0.1	Max 0.05	Max 0.25	Max 0.15	Max 0.05	

Table 2
Mechanical properties obtained from tensile test for AA 2024-T3.

Young's modulus, E	73GPa
Yield strength (0.2% proof), S_y	337 MPa
Tensile strength, S_u	471 MPa
Break elongation	17.5%

Notches were machined on each 25 × 90 mm slab using electrical discharge machining (EDM), a process selected for its high precision and minimal residual stress introduction. Following EDM, the notch surfaces were polished with fine-grit emery papers (#1200 to #1500) to remove any residual contamination. To verify dimensional accuracy, notch dimensions were inspected at magnifications ranging from 50× to 200× after each processing step.

Fatigue tests were conducted under load-controlled conditions using a Zwick/Roell servo-hydraulic fatigue testing machine at ambient laboratory temperature, in accordance with ASTM E466 [43]. Prior to the fatigue testing, each specimen was subjected to a single tensile overload cycle of sufficient magnitude to induce a residual stress field. All tests were conducted under a nominal stress ratio with R_{nom}=-1 and a frequency range of 20-30 Hz (verified not to affect results [43]). Crack detection was performed using optical microscopy at magnifications ranging from 150× to 200×. The assembled fatigue specimen mounted in the testing machine and a cracked sample are shown in Fig. 4.

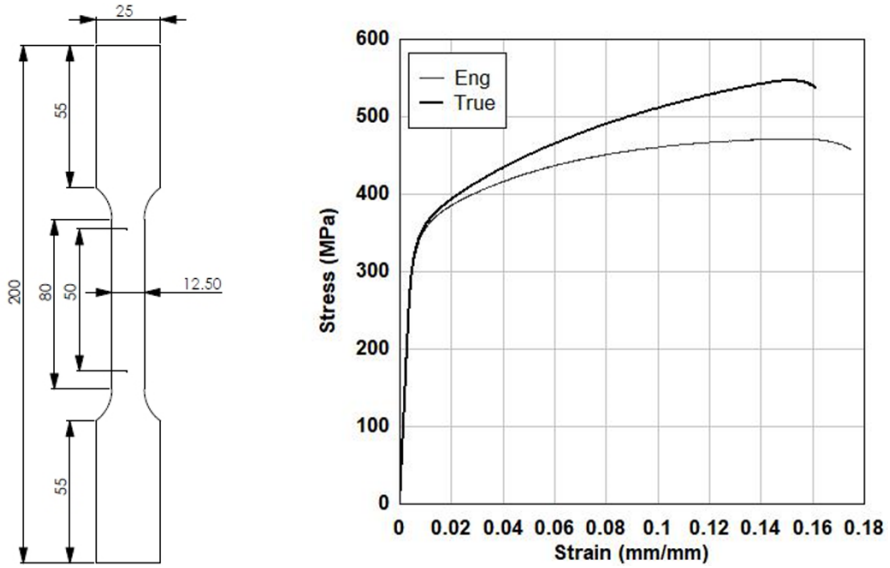

Fig. 3. The standard tensile test specimen and the stress-strain curve of AA 2024-T3.

Fig. 4. The assembled specimen on the testing machine and a cracked sample.

The loading conditions were systematically varied to investigate multiple scenarios for each notch configuration. Complete experimental details are provided in Table 3.

3. Application of Numerical Method

Advances in numerical computation over the past two decades have significantly enhanced the effectiveness of characteristic length methods. The inherent simplicity of these methods has become particularly advantageous with modern computational capabilities, powerful computing systems now enable highly accurate and efficient calculation of stress parameters at each point of interest.

In this study, finite element (FE) analysis was employed to compute stress distributions around the notch root, which play a critical role in the model. All simulations were conducted using Abaqus commercial software in three-dimensional space, as the hot spot was modeled at the specimen's mid-plane in close proximity to the notch root.

Table 3
Details of loading conditions and effective stress parameters.

Code	Plastic Overload (MPa)	Fatigue(MPa)	σ_m(MPa)	$\sigma_{a,eff}$(MPa)	K_G(MPa/MPa)
U5-01	150	133.3	-18.35	332.04	1.0796
U5-02	150	106.7	-40.83	282.24	1.0577
U5-03	150	80	-45.73	214.20	1.0535
U5-04	200	160	-39.35	338.86	1.1546
U5-05	200	133.3	-70.38	302.37	1.1195
U5-06	200	106.7	-108.71	260.73	1.0871
U5-07	200	80	-155.22	212.07	1.0569
U5-08	250	186.7	-58.75	350.17	1.2348
U5-09	250	160	-86.07	316.81	1.1958
U5-10	250	133.3	-118.13	279.66	1.1599
U5-11	250	106.7	-156.30	238.33	1.1269
U5-12	250	80	-201.94	191.40	1.0958
V60R0.4-01	100	93.3	-20.19	468.58	0.9170
V60R0.4-02	100	80	-48.42	423.19	0.8924
V60R0.4-03	100	66.7	-81.78	372.89	0.8691
V60R0.4-04	100	53.3	-121.55	316.50	0.8466
V60R0.4-05	100	40	-168.83	253.76	0.8249
V60R0.4-06	150	106.7	-90.47	454.50	1.0203
V60R0.4-07	150	93.3	-118.77	412.00	0.9935
V60R0.4-08	150	80	-149.43	366.39	0.9692
V60R0.4-09	150	66.7	-182.75	317.22	0.9464
V60R0.4-10	150	53.3	-219.61	263.63	0.9249
V60R0.4-11	200	106.7	-176.12	399.42	1.1454
V60R0.4-12	200	93.3	-204.94	359.30	1.1132
V60R0.4-13	200	80	-234.79	316.73	1.0846
V60R0.4-14	200	66.7	-265.38	271.29	1.0592
V60R0.4-15	200	53.3	-296.51	222.49	1.0367
V30R0.2-01	50	40	-41.74	371.56	0.9581
V30R0.2-02	50	33.3	-67.02	323.94	0.9206
V30R0.2-03	50	26.7	-84.38	267.63	0.8990
V30R0.2-04	50	20	-108.12	208.51	0.8721
V30R0.2-05	75	40	-122.87	326.55	1.0950
V30R0.2-06	75	33.3	-161.17	283.56	1.0444
V30R0.2-07	75	26.7	-195.82	237.61	0.9980
V30R0.2-08	75	20	-233.52	186.32	0.9557
V30R0.2-09	100	40	-202.89	289.50	1.2943
V30R0.2-10	100	33.3	-232.95	248.81	1.2316
V30R0.2-11	100	26.7	-264.59	206.03	1.1765
V30R0.2-12	100	20	-299.33	159.66	1.1258
V30R0.2-13	100	13.3	-338.22	110.13	1.0769

The mesh was specifically refined near the notch root to improve computational accuracy in this critical region, following established procedures [44]. Element dimensions in the notch root area were reduced to a minimum of 10μm. The model utilized eight-node brick elements with reduced integration (C3D8R) throughout the notch-affected zone and beyond. Material elastic-plastic behavior was implemented in the software based on the experimental stress-strain curve, following the software's guidelines [45]. A sample of the finite element model, the refined elements around the notch root, and the distribution of residual stresses under different overloads are shown in Fig. 5. This figure also illustrates the effects of the number of elements and nodes on the results for a 100MPa overload. It can be observed that with more than about 5000 elements and nodes, the results become sufficiently accurate.

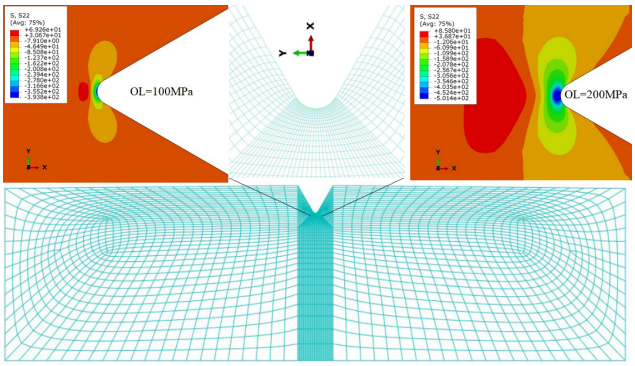

(a)

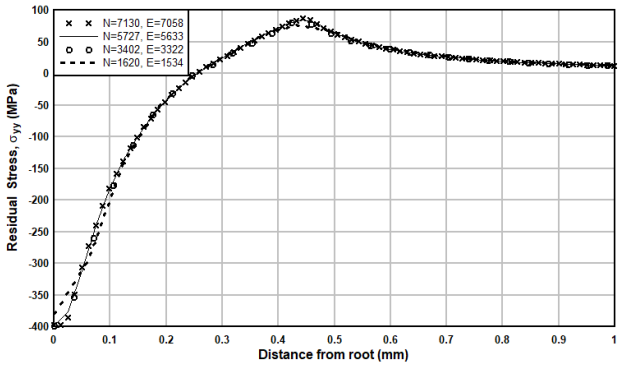

(b)

Fig. 5. a) Finite element model and induced residual stress under various Ols. b) Effects of number of elements (E) and nodes (N) on the results for 100 MPa OL.

4. Results and Discussion

To evaluate the accuracy and validity of the proposed model, this section presents a comparative analysis between predicted and experimental results. The characteristic length for each specimen was computed using FE analysis according to the given explanations in section 2.1 and 4. Then, the effective stress amplitude ($\sigma_{a,eff}$) was computed at the hot spot, with results presented in Table 3.

The stress concentration factor (K_G) was calculated using Eq. 5, where it is appropriately treated as a function of the characteristic length (a_ν), consistent with the theoretical framework established in Section 2.3.

$$K_G\left(a_v\right) = C_1 a_v + C_2 \tag{4}$$

The constants C1 and C2, which represent geometric parameters, were determined through calibration using at least two different tests on similar specimens. Optimal values for each notch configuration are provided in Table 4.

Table 4
Geometrical constants for different notch series.

	U5	V60R0.4	V30R0.2
SCF	2.45	5.55	8.25
C_1	-0.140268	-1.829979	-7.793242
C_2	0.953120	1.308174	1.199083

To ensure methodology independence from failure definition, surface cracks of varying lengths were considered as the failure criteria for each notch series: U5 series with 1.1mm, V60R0.4 series with 0.6mm, and V30R0.2 series with 0.1mm.

These values were lower than the largest characteristic length of each notch series. The corresponding number of cycles to failure (N_f) was estimated using the material's S-N curve (Fig. 6) from Reference [46], with σ_a as the input parameter.

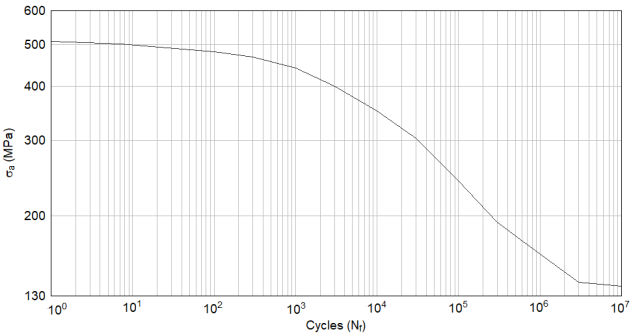

Fig. 6. he S-N curve of AA 2024-T3 [46].

The results of the analysis are presented graphically in Fig. 7, which plots experimentally measured cycles to failure (N_f) versus predicted values ($N_{f,p}$). To assess prediction accuracy, each notch series plot includes two parallel bands flanking the line of exact estimation (N_f=$N_{f,p}$). The results demonstrate remarkable agreement between predicted and experimental values in most cases, confirming the validity and accuracy of the model.

There are several reasons why significant differences often exist between experimental and numerical or analytical results in the fatigue life estimation of metals:

- Material variability: Real materials have microstructural imperfections, inclusions, and residual stresses that are difficult to fully account for in numerical models. These factors can significantly affect fatigue behavior.
- Simplifications in modeling: Numerical and analytical methods often involve assumptions and simplifications (e.g., linear elasticity, idealized loading conditions, perfect geometry) that do not perfectly reflect real-world conditions.
- Environmental and loading conditions: Experimental results are influenced by actual testing conditions such as temperature, humidity, loading frequency, and surface finish, which may not be accurately represented in simulations.
- Crack initiation and propagation: Many models focus either on crack initiation or crack growth, while experimental results typically reflect the total fatigue life. This difference in focus can lead to discrepancies.
- Scatter in experimental data: Fatigue life inherently has a high degree of variability, even under identical conditions. This scatter leads to a wide range of experimental results, making it challenging to match them with precise numerical predictions.

A detailed examination of the results, particularly for the V30R0.2 notch series, reveals that the model exhibits a slight tendency to underestimate fatigue life. From an engineering design perspective, this conservative prediction can be considered as advantageous, as it aligns with the common practice of considering worst-case scenarios. Notably, the model demonstrates remarkable accuracy for extremely sharp notches (SCF=8.25), where higher stress gradients near the notch root would typically lead to prediction instability. This performance is particularly significant given the challenging conditions presented by such severe stress concentrations.

The enhanced accuracy observed for the V30R0.2 notch series can be attributed to the model's improved capability in characterizing geometric effects on the hot spot length when in close proximity to the notch root. This suggests that model accuracy may be further refined through the implementation of higher-order functions for estimating the geometric factor (K_G). The demonstrated adaptability of the hot spot approach indicates its potential applicability to other residual stress field scenarios, including those induced by thermal loading conditions. Notably, the model maintained consistent prediction accuracy across a broad fatigue life range (10^3 to 10^6 cycles), demonstrating effectiveness in both medium-cycle fatigue (MCF) and high-cycle fatigue (HCF) regimes. However, further investigation is required to assess model performance under low-cycle fatigue (LCF) conditions.

Table 5 presents the estimation errors for σ_a across different notch series. The results demonstrate that 77.5% of predictions showed less than 10% error , while 92.5% of the predictions remained within 20% error. These findings confirm that the hot spot model provides accurate predictions for both hot spot location identification and effective stress parameter determination.

To evaluate the geometric influence on prediction accuracy, Fig. 8 presents the σ_a results for each notch series. The plot contains two distinct data sets: "Effective stress" points represent (N_f, σ_{ff}) pairs and "prediction" points show ($N_{f,p}$, σ_a) pairs.

The results presented in this section provide strong support for the validity of the model. The good agreement between the predictions and experimental data suggests that the proposed model can effectively capture certain microstructural phenomena, though further investigation through mechanistic modeling is warranted. Based on these findings, we propose that this model could be extended to other residual stress fields, including weldments and shot-peened components, since the hot-spot length derivation accounts for plastic strain effects.

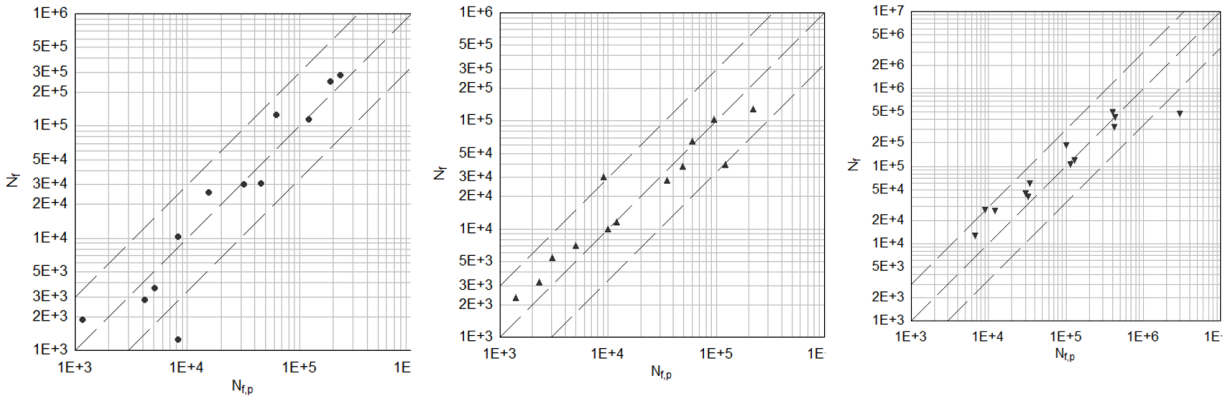

(a) U5 (b) V60R0.4 (c) V30R0.2

Fig. 7. Comparison of the predicting fatigue lives ($N_{f,p}$) with experimental data (N_f).

Table 5
Estimation errors of σ_a for different notch series.

Code	σ_a (MPa)		Error (%)
	Prediction	Measured	
U5-01	358	495	-27.67
U5-02	298	281	6.05
U5-03	225	234	-3.85
U5-04	391	400	-2.25
U5-05	338	317	6.62
U5-06	283	296	-4.39
U5-07	224	200	12.00
U5-08	432	418	3.35
U5-09	378	393	-3.82
U5-10	324	351	-7.69
U5-11	268	235	14.04
U5-12	209	198	5.55
V60R0.4-01	429	410	4.63
V60R0.4-02	377	365	3.29
V60R0.4-03	324	303	6.93
V60R0.4-04	267	269	-0.74
V60R0.4-05	209	220	-5.00
V60R0.4-06	463	439	5.47
V60R0.4-07	409	396	3.28
V60R0.4-08	355	355	0.00
V60R0.4-09	300	313	-4.15
V60R0.4-10	243	248	-2.02
V60R0.4-11	457	431	6.03
V60R0.4-12	399	372	7.26
V60R0.4-13	343	349	-1.72
V60R0.4-14	287	296	-3.04
V60R0.4-15	230	297	-22.56
V30R0.2-01	355	316	12.34
V30R0.2-02	298	284	4.93
V30R0.2-03	240	242	-0.83
V30R0.2-04	181	186	-2.69
V30R0.2-05	357	309	15.53
V30R0.2-06	296	272	8.82
V30R0.2-07	237	242	-2.07
V30R0.2-08	178	179	-0.56
V30R0.2-09	374	338	10.65
V30R0.2-10	306	286	6.99
V30R0.2-11	242	241	0.41
V30R0.2-12	179	177	1.13
V30R0.2-13	118	200	-41.00

The term “hot spot” proves particularly appropriate, as it conceptually represents:

- The fatigue behavior of the plastic zone
- An effective entity resulting from plastic deformation, though not physically observable
- The hot-spot model demonstrates notable advantages in terms of:
- Predictive accuracy
- Numerical stability
- Computational efficiency

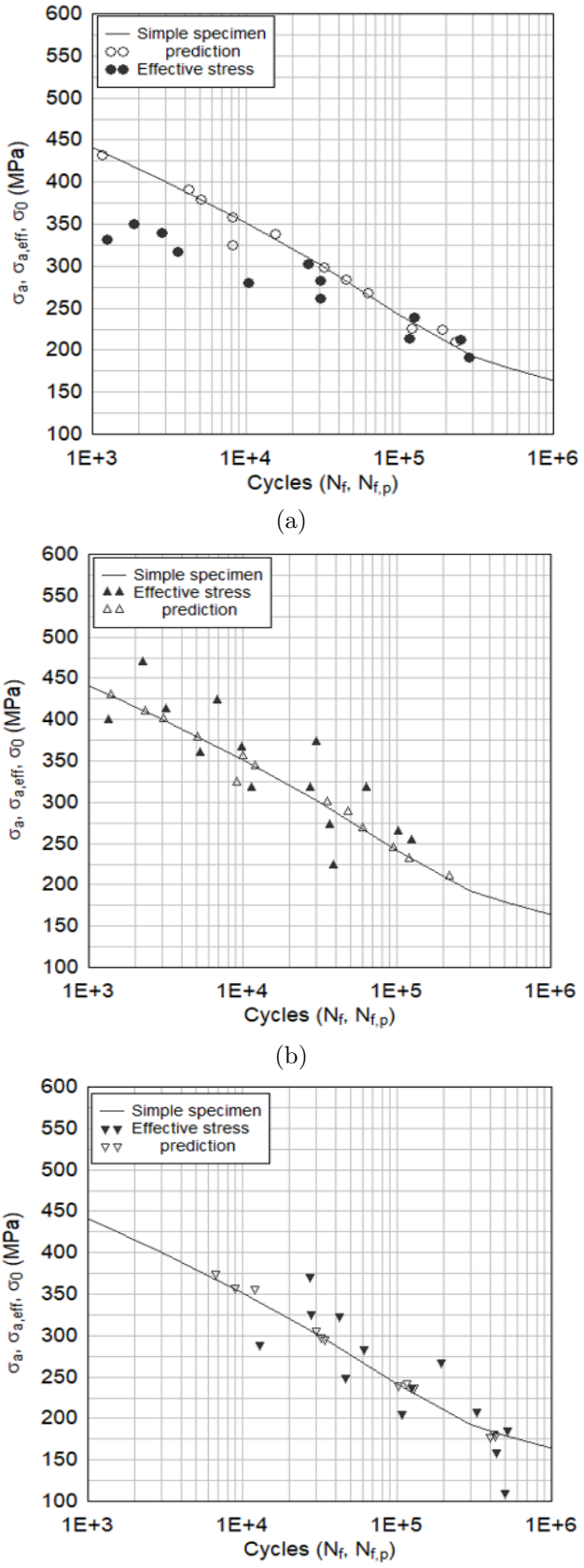

Fig. 8. Effective stress parameter influence on fatigue failure and model prediction for notch series of a) U5, b) V60R0.4 and c) V30R0.2.

These characteristics position the hot spot approach as a potentially powerful tool for engineering design applications. Furthermore, the model's framework appears sufficiently robust to allow extensions beyond crack initiation, potentially bridging the gap between the traditionally separate domains of fatigue research (initiation and propagation).

The present model requires only a limited number of experimentally measured parameters, with the potential to further reduce experimental requirements in future studies. Notably, the majority of parameters used in this investigation were derived from standardized tests on plain specimens' data that are commonly available in the literature for various materials.

5. Conclusions

A concept hot spot model incorporating local stress ratio (R_{local}) was developed to predict fatigue life in notched components with residual stress fields near the notch root. The model's validity and accuracy were verified through comprehensive experimental testing on multiple notched specimen configurations. Results demonstrate the model's effectiveness, offering both computational simplicity and predictive accuracy, making it particularly valuable for analyzing complex fatigue conditions involving residual stress fields. Based on the experimental and analytical results, the following key conclusions can be drawn:

1) The presence of compressive residual stresses near the notch root significantly enhances the fatigue life of notched components. This phenomenon can be effectively predicted using the proposed model.

2) The proposed model maintains consistent accuracy even for components with high stress concentration factors. This suggests the model remains applicable, with potential refinements during the crack initiation phase for investigating small crack growth behavior in the residual stress fields.

3) The hot-spot model represents a methodological approach to account for plastic strain effects in stress concentration zones when predicting fatigue failure.

4) Further investigation is required to validate the accuracy of the model under residual stress fields induced by welding or other manufacturing processes. Additionally, comprehensive studies should be conducted to assess the model's reliability under multiaxial loading conditions and variable amplitude loading scenarios.

References

[1] E. Santecchia, A. Hamouda, F. Musharavati, E. Zalnezhad, M. Cabibbo, M. El Mehtedi, S. Spigarelli, A review on fatigue life prediction methods for metals, Adv. Mater. Sci. Eng., (2016) 9573524.

[2] K. Zakaria, S. Abdullah,M. Ghazali, A Review of the Loading Sequence Effects on the Fatigue Life Behaviour of Metallic Materials, J. Eng. Sci. Technol. Rev., 9(5) (2016) 189-200.

[3] J. E. Shigley, Shigley's mechanical engineering design, Tata McGraw-Hill Education, (2011).

[4] D. Taylor, The theory of critical distances: a new perspective in fracture mechanics, Elsevier, (2010).

[5] H. Neuber, Theory of notch stresses: principles for exact calculation of strength with reference to structural form and material. Vol. 4547. USAEC Office of Technical Information, (1961).

[6] R. E. Peterson, Notch sensitivity, Metal Fatigue, (1959) 293-306.

[7] L. Susmel, Multiaxial Notch Fatigue, Elsevier, (2009).

[8] H. Adib, J. Gilgert, G. Pluvinage, Fatigue life duration prediction for welded spots by volumetric method, Int. J. Fatigue, 26(1) (2004) 8194.

[9] M. El Haddad, K. Smith, T. Topper, Fatigue crack propagation of short cracks, J. Eng. Mater. Technol., 101(1) (1979) 42-46.

[10] G. Qylafku, Z. Azari, N. Kadi, M. Gjonaj, G. Pluvinage, Application of a new model proposal for fatigue life prediction on notches and key-seats, Int. J. Fatigue, 21(8) (1999) 753-760.

[11] L. Susmel, D. Taylor, Estimating Lifetime of Notched Components Subjected to Variable Amplitude Fatigue Loading According to the Elastoplastic Theory of Critical Distances, J. Eng. Mater. Technol., 137(1) (2015) 011008.

[12] R. Seifi, M. R. Mohammadi, Fatigue Life Prediction of Notched Components after Plastic Overload Using Theory of Critical Distance, J. Stress Anal., 5(2) (2021) 1120.

[13] D. Gao, W. Yao, W. Wen, J. Huang, Critical distance model for the fatigue life analysis under low-velocity impacts of notched specimens, Int. J. Fatigue, 146 (2021) 106164.

[14] R. Seifi, M. R. Mohammadi, Fatigue life estimation of the overloaded notched components, J. Braz. Soc. Mech. Sci. Eng., 42(1) (2019) 51.

[15] A. Khanna, J. Vidler, M. Bermingham, A. Sales, L. Yin,A. Kotousov, A compliance-based method for correcting fatigue crack growth data in the presence of residual stresses, Int. J. Fatigue, 199 (2025) 109066.

[16] P. Ferro, F. Berto, S. M. J. Razavi, M. R. Ayatollahi, The effect of residual stress on fatigue behavior of V-notched components: a review, Procedia Struct. Integr., 3 (2017) 119125.

[17] X. Xiao, V. Okorokov,D. Mackenzie, High cycle fatigue life assessment of notched components with induced compressive residual stress, Int. J. Press. Vessel. Pip., 206 (2023) 105069.

[18] Ž. Božić, S. Schmauder,H. Wolf, The effect of residual stresses on fatigue crack propagation in welded stiffened panels, Eng. Fail. Anal., 84 (2018) 346357.

[19] A. M. Mirzaei, A. H. Mirzaei, A. Sapora, P. Cornetti, Strain based finite fracture mechanics for fatigue life prediction of additively manufactured samples,Int. J. Fract., 249(3) (2025) 44.

[20] T. Gao, Y. Tong, Z. Zhan, W. Mei, W. Hu, Q. Meng, Development of a non-local approach for life prediction of notched specimen considering stress/strain gradient and elastic-plastic fatigue damage, Int. J. Damage Mech., 31(7) (2022) 10571081.

[21] S. Wu, J. Liu, J. Lu, Y. Wang, W. Kou, Fatigue life evaluation of notched components affected by multiple factors, Arch. Appl. Mech., 94(7) (2024) 18711889.

[22] J. Liu, X. Pan, Y. Li, X. Chen, A Two-point Method for Multiaxial Fatigue Life Prediction, Acta Mech. Solida Sin., 35(2) (2022) 316327.

[23] C. Zhang, R. Wan, J. He, J. Yu, A multiaxial fatigue life analysis method for automotive components based on LSTM-CNN, Int. J. Fatigue, 199 (2025) 109062.

[24] D. Wang, J.Hogan, L. Lamborn, Safe Life of Line Pipe in Hydrogen Blended Transport. In Pressure Vessels and Piping Conference (Vol. 87448, p. V001T01A024), Am. Soc. Mech. Eng., (2023, July).

[25] G. E. Varelis, A. Briffett, H. Latif, T. Papatheocharis,L. Bernardi, Design Considerations for Hydrogen Pipelines, J. Press. Vessel Technol., 147(5) (2025).

[26] T. Prewitt, S. Esmaeely, Hydrogen Storage Lifecycle Assessment. In Pressure Vessels and Piping Conference (Vol. 88483, p. V002T03A111). Am. Soc. Mech. Eng., (2024, July).

[27] M. Fartas, S. Fouvry, P. Arnaud, S. Garcin, F. Pires, Prediction of fretting fatigue damage under variable loading blocks: Effect of plasticity, Int. J. Fatigue, 199 (2025) 109022.

[28] R. Shi, D. Wei, S. Yang, A stress fatigue lifeprediction model applicable to the whole life stage and complex stress states, Chin. J. Aeronaut., 38(6) (2025) 103412.

[29] Y. Shen, J. Huang, Residual life forecasting and advanced surface damage remanufacturing processes for automotive drive axle shells, Adv. Mech. Eng., 17(2) (2025) 16878132251321054.

[30] W. Wang, H. Liu, C. Zhu, X. Du, J. Tang, Effect of the residual stress on contact fatigue of a wind turbine carburized gear with multiaxial fatigue criteria, Int. J. Mech. Sci., 151 (2019) 263-273.

[31] M. Ciavarella,F. Monno, A comparison of multiaxial fatigue criteria as applied to rolling contact fatigue, Tribol. Int., 43(11) (2010) 21392144.

[32] M. Benedetti,C. Santus, Mean stress and plasticity effect prediction on notch fatigue and crack growth threshold, combining the theory of critical distances and multiaxial fatigue criteria, Fatigue Fract. Eng. Mater. Struct., 42(6) (2019) 12281246.

[33] D. Taylor, Geometrical effects in fatigue: a unifying theoretical model, Int. J. Fatigue, 21(5) (1999) 413420.

[34] S. Vantadori, J. V. Valeo, A. Zanichelli, Fretting fatigue and shot peening: a multiaxial fatigue criterion including residual stress relaxation, Tribol. Int., 151 (2020) 106537.

[35] J. F. Flavenot, N. Skalii, A comparison of multiaxial fatigue criteria incorporating residual stress effects, in International Conference on Biaxial/Multiaxial Fatigue and Fracture (ICBMFF2). (2013).

[36] J. Flavenot, N. Skalli. A Critical Depth Criterion for the Evaluation of Long Life Fatigue Strength under Multiaxial Loading and a Stress Gradient, in International Conference on Biaxial/Multiaxial Fatigue and Fracture (ICBMFF2). (2013).

[37] R. Rice, J. Jackson, J. Bakuckas, S. Thompson, Metallic Materials Properties Development and Standardization (MMPDS) Handbook, NTIS Virginia Scientific Report, (2003).

[38] M. J. Caton, R. John, W. J. Porter, M. Burba, Stress ratio effects on small fatigue crack growth in Ti6Al4V, Int. J. Fatigue, 38 (2012) 36-45.

[39] R. I. Stephens, D. K. Chen, B. W. Hom, Fatigue Crack Growth with Negative Stress Ratio Following Single. In Fatigue Crack Growth Under Spectrum Loads: A Symposium Presented at the Seventy-eighth Annual Meeting, American Society for Testing and Materials, Montreal, Canada, 23-24 June, 1975, RP Wei and RI Stephens, Symposium Cochairmen (Vol. 595, p. 27) (1976). ASTM.

[40] A. Association, International alloy designations and chemical composition limits for wrought aluminum and wrought aluminum alloys, Arlington, VA: The Aluminum Association, (2009).

[41] E. ASTM, 112-96. (2004). Standard test methods for determining average grain size, ASTM International: West Conshohocken, PA, USA, (2004).

[42] A. Standard, E8, Standard Test Methods for Tension Testing of Metallic Materials, Annual book of ASTM standards, 3 (2004) 5772.

[43] A. Standard, E466: Standard Practice for Conduction Force Controlled Constant Amplitude Axial Fatigue Test of Metallic Materials, vol. 03.01, Annual Book of ASTM Standards, West Conshohocken, (2002).

[44] M. Benedetti, V. Fontanari, C. Santus,M. Bandini, Notch fatigue behaviour of shot peened high-strength aluminium alloys: Experiments and predictions using a critical distance method, Int. J. Fatigue, 32(10) (2010) 16001611.

[45] H. Hibbitt, B. Karlsson, P. Sorensen, Abaqus Analysis Users Manual Version 2016, Dassault Systmes Simulia Corp, Providence, (2016).

[46] W. Illg, Fatigue tests on notched and unnotched sheet specimens of 2024-T3 and 7075-T6 aluminum alloys and of SAE 4130 steel with special consideration of the life range from 2 to 10,000 cycles, (1956) NASA Technical Reports Server.